

This is the peer reviewed version of the following article:

Ce-exchange capacity of zeolite L in different cationic forms: a structural investigation / Confalonieri, G; Vezzalini, G; Quattrini, F; Quartieri, S; Dejoie, C; Arletti, R. - In: JOURNAL OF APPLIED CRYSTALLOGRAPHY. - ISSN 1600-5767. - 54:6(2021), pp. 1766-1774. [10.1107/S1600576721010827]

Terms of use:

The terms and conditions for the reuse of this version of the manuscript are specified in the publishing policy. For all terms of use and more information see the publisher's website.

18/12/2025 18:58

ARTICLE IN PRESS – J. Appl. Cryst.



JOURNAL OF
APPLIED
CRYSTALLOGRAPHY

ISSN 1600-5767

Ce-exchange capacity of zeolite L in different cationic forms: a structural investigation

Proof instructions

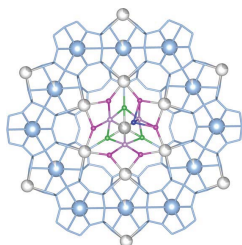
Proof corrections should be returned by **18 November 2021**. After this period, the Editors reserve the right to publish your article with only the Managing Editor's corrections.

Please

- (1) Read these proofs and assess whether any corrections are necessary.
- (2) Check that any technical editing queries highlighted in **bold underlined** text have been answered.
- (3) Send corrections by e-mail to **ls@iucr.org**. Please describe corrections using plain text, where possible, giving the line numbers indicated in the proof. Please do not make corrections to the pdf file electronically and please do not return the pdf file. If no corrections are required please let us know.



To arrange payment for **open access**, please visit <https://scripts.iucr.org/openaccess/?code=vb5024>. To purchase printed offprints, please complete the attached order form and return it by e-mail.

Please check the following details for your article



Thumbnail image for contents page

Synopsis: Zeolite L was Na- and NH₄-exchanged and the resulting samples were characterized by structural and chemical analyses. From the perspective of the possible use of zeolite L for rare earth element recovery (in particular Ce) and to unveil the differences in the affinity for Ce dictated by the presence of different counter-cations, the three samples with LTL framework type were Ce³⁺-exchanged and fully characterized.

Abbreviated author list: Confalonieri, G.; Vezzalini, G.; Quattrini, F.; Quartieri, S. ( 0000-0001-5646-8057); Dejoie, C. ( 0000-0003-3313-3515) Arletti, R.

Keywords: Ce-exchanged zeolite; structural analysis; synchrotron high-resolution X-ray powder diffraction

Licence to publish: Licence to publish licence agreed.

How to cite your article in press

Your article has not yet been assigned page numbers, but may be cited using the doi:

Confalonieri, G., Vezzalini, G., Quattrini, F., Quartieri, S., Dejoie, C. & Arletti, R. (2022). *J. Appl. Cryst.* **55**, <https://doi.org/10.1107/S1600576721010827>.

You will be sent the full citation when your article is published and also given instructions on how to download an electronic reprint of your article.



Received 3 August 2021

Accepted 19 October 2021

Edited by H. Brand, Australian Synchrotron,
ANSTO, Australia**Keywords:** Ce-exchanged zeolite; structural
analysis; synchrotron high-resolution X-ray
powder diffraction.**Supporting information:** this article has
supporting information at journals.iucr.org/j

Ce-exchange capacity of zeolite L in different cationic forms: a structural investigation

Giorgia Confalonieri,^{a,*} Giovanna Vezzalini,^b Filippo Quattrini,^b Simona Quartieri,^b Catherine Dejoie^a and Rossella Arletti^b

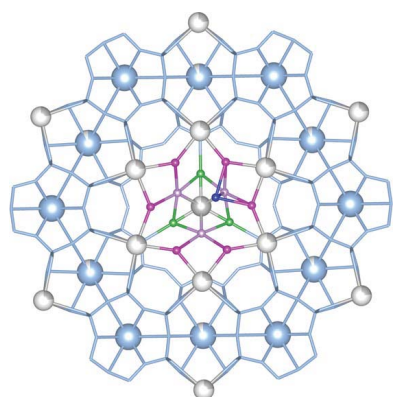
^aID22 Beamline, European Synchrotron Radiation Facility (ESRF), 71 Avenue des Martyrs, Grenoble, 38000, France, and^bDipartimento di Scienze Chimiche e Geologiche, Università degli Studi di Modena e Reggio Emilia, Modena, Italy.

*Correspondence e-mail: giorgia.confalonieri@esrf.fr

Cerium exchange by microporous materials, such as zeolites, has important applications in different fields, for example, rare earth element recovery from waste or in catalytic processes. This work investigated the Ce-exchange capacity of zeolite L in three different cationic forms (the as-synthesized K form and Na- and NH₄-exchanged ones) from a highly concentrated solution. Chemical analyses and structural investigations allowed determination of the mechanisms involved in the exchanges and give new insights into the interactions occurring among the cations and the zeolite framework. Different cation sites are involved: (i) K present in the original LTL in the cancrinite cage (site KB) cannot be exchanged; (ii) the cations in KD (in the 12-membered ring channel) are always exchanged; while (iii) site KC (in the eight-membered ring channel) is involved only when K⁺ is substituted by NH₄⁺, thus promoting a higher exchange rate for NH₄⁺ → K⁺ than for Na⁺ → K⁺. In the Ce-exchanged samples, a new site occupied by Ce, in the centre of the main channel, appears, accompanied by a rearrangement of the H₂O molecules and an **increase in the number of H₂O molecules [ok as edited?]**. In terms of Ce exchange, the three cationic forms behave similarly, from both the chemical and structural point of view (exchanged Ce ranges from 38 to 42% of the pristine cation amount). Beyond the intrinsic structural properties of the zeolite L framework, the Ce exchange seems thus also governed by the water coordination sphere of the cation. Complete Ce recovery from zeolite **pores** was achieved.

1. Introduction

The scarcity of rare earth elements (REE) in some regions, such as Europe (Massari & Ruberti, 2013; Charalampides *et al.*, 2015), and the well known balance problem (*i.e.* the balance between natural abundance and market request) (Binnemans *et al.*, 2018; de Boer & Lammertsma, 2013) are pushing the scientific community to find alternative ways to supply REE. The most promising solution is to recycle them from waste, which in the last few years has become an urgent requirement for society (Jowitt *et al.*, 2018; Rademaker *et al.*, 2013; Balaram, 2019). Beyond the economic benefits, this process is also necessary for the ecological preservation of the natural environment (Balaram, 2019). The mining, extraction and refining of these **REE?** elements are in fact associated with high environmental costs (Charalampides *et al.*, 2016; Haque *et al.*, 2014). Despite the fact that eco-friendly politics is supportive of and encourages the development of recycling solutions, the current REE recovery percentage is still lower than 1%, and is limited to a few and very specific applications such as recovery from magnets and polishing compounds (Chakhmouradian & Wall, 2012; Royen & Fortkamp, 2016). The goal for the near future is, thus, to increase the REE



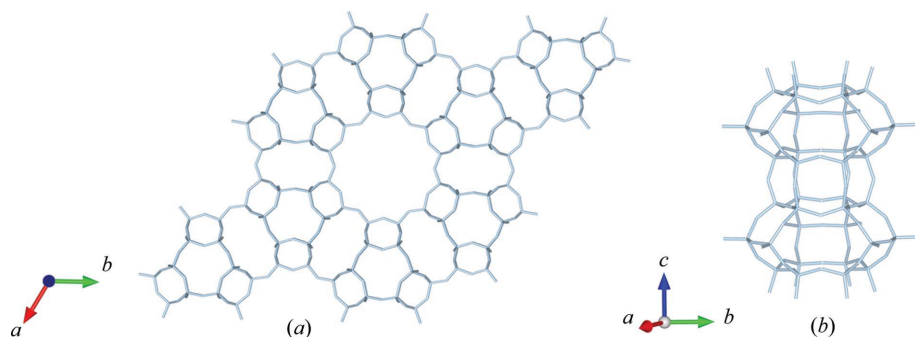


Figure 1
(a) LTL framework type; (b) columns constituting the framework, formed by the stacking of cancrinite cages and double six-membered rings.

recycling rate by finding an economical and convenient way to recover these elements from waste. Leached liquors obtained from waste can be a rich secondary source of REE and many methods have been tested to recover them, *i.e.* solvent extraction (Meshram & Abhilash, 2020; Deshmane *et al.*, 2020; Ni'Am *et al.*, 2020), precipitation (Zhou *et al.*, 2018; Porvali *et al.*, 2018; Diaz *et al.*, 2016), ion exchange (Royen & Fortkamp, 2016). The latter can exploit various materials such as active carbon (Gad & Awwad, 2007), resins (Manos & Kanatzidis, 2016) or microporous materials (Kavun *et al.*, 2021; Royen & Fortkamp, 2016) such as zeolites.

Zeolites are natural and synthetic microporous materials mainly constituted by a complex interconnection of SiO_4 and AlO_4 tetrahedra which leads to many different types of framework (Baerlocher *et al.*, 2007; Baeloche & McCusker iza-structure database <http://www.iza-structure.org/databases/>) and pore systems (*i.e.* cages, 1D, 2D and 3D network channels). The zeolite **pores**, thanks to their nanometric sizes, can host water molecules (Bryukhanov *et al.*, 2017; Coudert *et al.*, 2009; Saada *et al.*, 2011; Bennett & Smith, 1968), many different types of cations (Arletti *et al.*, 2017 [two Arletti *et al.* 2017 references, please indicate which]; Confalonieri *et al.*, 2018, 2020 [three Confalonieri *et al.* 2020 references, please indicate which]; Frising & Leflaive, 2008; Isaac *et al.*, 2020; Simoncic & Armbruster, 2004; Barrer & Meier, 1958; Bennett & Smith, 1968) and/or organic molecules [including CO_2 (Hong *et al.*, 2014; Hudson *et al.*, 2012; Lu *et al.*, 2008; Confalonieri *et al.*, 2020), alcohol (Zhang *et al.*, 2012; Arletti *et al.*, 2017; Confalonieri *et al.*, 2019), various hydrocarbons (Fabbiani *et al.*, 2021; Confalonieri *et al.*, 2020; Santoro *et al.*, 2003, 2016; Scelta *et al.*, 2014), dyes (Dejoie *et al.*, 2014) or even amino acids (Boekfa *et al.*, 2008; Krohn & Tsapatsis, 2005; Stückenschneider *et al.*, 2013) *etc.*]. One of the most remarkable properties of zeolites is the high cationic exchange capacity, where cations in the pores can be easily exchanged (Pabalan & Bertetti, 2001; Dyer, 2007). Zeolites are green materials and cheap [to produce], and their high cationic exchange capacity could potentially be exploited for REE recovery; however, only a few works have investigated this possibility (Mosai *et al.*, 2019; Faghihian *et al.*, 2005; Duploux, 2016; Barros *et al.*, 2019), and thus new and extensive studies are desirable.

In this paper, we describe a preliminary test of the effectiveness of different cationic forms of zeolite L (LTL framework type) (Baerlocher *et al.*, 2007) for cerium recovery. This framework type has been reported as suitable for REE recovery (Duploux, 2016), and Ce is one of the most exploited REE in terms of volume (Binnemans *et al.*, 2018; Charalampides *et al.*, 2015), being present in a huge variety of technological applications [*i.e.* as fluid catalytic cracking (f.c.c.) catalysts, glass polishing, fluorescent lamps, NiMH batteries *etc.* (Meshram & Abhilash, 2020)]. We examine the use of

synthetic zeolite L in its as-synthesized K form and in the Na- and NH_4 -exchanged ones. The three cationic forms are tested in experiments of Ce exchange from a highly concentrated solution. The obtained results contribute to our understanding of whether zeolite L is suitable for Ce exchange and recovery, and whether Ce shows a different affinity for the diverse exchanged forms. The study was carried out by a combination of different techniques, including structural refinement of high-resolution X-ray powder diffraction experiments. The exploitation of zeolites as cation exchangers cannot disregard the mechanisms involved in the exchanges and the interaction occurring among extra-framework cations, framework and H_2O molecules. Thus, a structural study unravelling from the atomistic point of view the cation exchange mechanism and the sites involved is fundamental for the choice of a powerful protocol of exchange. Indeed, the determination, from chemical analysis, of the maximum amount of Ce incorporated into the zeolite **pores** would give only a partial result since it would not shed light on the dynamics of Ce adsorption. Structural analyses reported here are fundamental to determine the interactions between Ce cations and the zeolite framework, and will pave the way to further studies devoted to the investigation of zeolite selectivity towards Ce. This structural interpretation can be exploited for targets other than REE recovery – for example, Ce-exchanged zeolites are very promising catalysts for the selective catalytic reduction of N_2O (van Kooten *et al.*, 1998) or for the sterification of glycerol with acetic acid (Gautam *et al.*, 2020).

2. Materials and methods

2.1. Zeolite L

Zeolite L [$\text{K}_6\text{Na}_3(\text{H}_2\text{O})_{21}\text{Al}_9\text{Si}_{27}\text{O}_{72}$, $a = 18.4$, $c = 7.52$ Å, $\gamma = 120^\circ$ (Baerlocher *et al.*, 2007)] (LTL framework type) (Fig. 1) is built by the linking of columns formed by the stacking of cancrinite cages and double six-membered rings (6MR), leading to the formation of a 1D porous system formed from [12-membered ring] 12MR and [eight-membered ring] 8MR channels running along the c axis. The structure is described using the $P6/mmm$ space group. In zeolite L, three sites,

named KB, KC and KD, are occupied by cations (Gigli *et al.*, 2013). KB is placed at the centre of the cancrinite cage, KC at the centre of the elliptical 8MR channel, while KD is close to the wall of the 12MR channel.

In the present work zeolite L, purchased from the Tosoh Corporation (Japan) in its K form (from now on termed K-LTL), was initially characterized and used as starting material for the ion-exchange experiments.

2.2. Ion-exchange experiments

2.2.1. Na^+ and NH_4^+ exchange experiments. With the purpose of obtaining different cationic forms, K-LTL was ion-exchanged with two solutions, containing Na^+ and NH_4^+ ions. The two solutions were prepared by dissolving NaNO_3 (sodium nitrate 99.5% RPE-ACS, Carlo Erba) and NH_4Cl (ammonium chloride 99.5% BAKER ANALYZED ACS, J. T. Baker) in double-distilled water, obtaining a 0.8 M concentration of sodium and ammonium. The high concentration of the two solutions was chosen to obtain the maximum exchange of the extra-framework cations of K-LTL.

The pristine sample was sieved so as to keep only particles with a uniform mesh size ($\geq 2.5 \mu\text{m}$), dried for 24 h at 60°C , and then put in contact with the two solutions under stirring for 5 days; the solution was changed every day to favour the ion-exchange process. The liquid/solid ratio was 16 ml/g, the temperature was set at 25°C and no buffer solution was used to control the pH to avoid interference in the exchange. Exchanged zeolites were rinsed three times with double-distilled water using an ALC multi-speed centrifuge PK 121 at 5000 r min^{-1} for 10 min and then dried for 24 h at 60°C . The cationic forms obtained in this way are labelled Na-LTL and $\text{NH}_4\text{-LTL}$. A second experiment was performed for sodium exchange at 80°C to evaluate the influence of temperature on the ion-exchange efficiency. The obtained sample is labelled Na-LTL- 80°C .

2.2.2. Ce^{3+} exchange and recovery. A Ce solution 0.48 M was prepared by dissolving $\text{Ce}(\text{NO}_3)_3 \cdot 6\text{H}_2\text{O}$ [cerium(III) nitrate hexahydrate, REacton, 99.5% (REO), Alfa Aesar] in double-distilled water. This concentration was chosen because it allows the number of Ce ions in the solution to be equal to three times the cation content of the zeolite, hence maximizing the Ce incorporation. The pristine K-LTL and samples Na-LTL and $\text{NH}_4\text{-LTL}$ were put in contact with the Ce solution (liquid/solid ratio = 20 ml/g) for 5 days at room temperature with no buffer solution. The solution was changed every day to favour the exchange. The samples were rinsed three times with double-distilled water using an ALC multi-speed centrifuge PK 121 at 5000 r min^{-1} for 10 min and then dried for 24 h at 60°C . The obtained zeolites are labelled K-Ce-LTL, Na-Ce-LTL and $\text{NH}_4\text{-Ce-LTL}$. For the last sample a further exchange, aimed at Ce recovery from the zeolite pores, was performed. $\text{NH}_4\text{-Ce-LTL}$ was put in contact with a solution $[\text{NH}_4^+] = 0.8 \text{ M}$ prepared by dissolving NH_4NO_3 (ammonium nitrate, 99%, Carlo Erba) in double-distilled water; it was left for 24 h under stirring, at room temperature. The obtained zeolite,

labelled $\text{NH}_4\text{-Ce-LTL-rev}$, was then rinsed as previously reported.

2.3. Analytical methods

Thermogravimetric analysis. Thermogravimetric analyses (TGA) were performed in the temperature range $25\text{--}1050^\circ\text{C}$ with a ramp of $10^\circ\text{C min}^{-1}$ under air flow, using a Seiko SSC/5200 thermal analyser. TGA were performed for all phases except Na-LTL- 80°C , for which the water content was determined by loss on ignition (LOI).

Elemental analysis. Elemental analyses (EA) were performed for samples $\text{NH}_4\text{-LTL}$ and $\text{NH}_4\text{-Ce-LTL}$ to evaluate nitrogen content. A Flash 2000 CHNS/MAS200R instrument, equipped with a highly sensitive thermal conductivity (TCD) detector, was used. FLASH dynamic combustion (modified Dumas method) allows a temperature of 1800°C to be reached, in order to release elementary gases from the samples.

X-ray fluorescence analysis. X-ray fluorescence (XRF) analyses of samples K-LTL and Na-LTL were performed using a wavelength-dispersive X-ray fluorescence Philips PW1480. Samples were ground and pressed with boric acid to obtain powder pellets. Data were collected and corrected on the basis of standard materials (Leoni & Saitta, 1976; Franzini *et al.*, 1975) and assuming the water content determined by LOI obtained by heating the powders in a furnace at 1000°C or by TGA.

Scanning electron microscopy with energy-dispersive spectroscopy (SEM-EDS). The chemical composition of samples exchanged with Ce (*i.e.* K-Ce-LTL, Na-Ce-LTL and $\text{NH}_4\text{-Ce-LTL}$) and $\text{NH}_4\text{-LTL}$ was checked using a scanning electron microscope Nova NanoSEM 450 equipped with an X-EDS Bruker QUANTAX-200 detector. Powders were compressed into thin self-supporting discs coated with gold. Chemical data were obtained by averaging the results obtained on five areas for each sample.

High-resolution X-ray powder diffraction (XRPD). Diffraction data were collected at ID22, the high-resolution beamline at the European Synchrotron Radiation Facility (ESRF), Grenoble, France, using the new Extremely Brilliant Source (EBS). The samples were ground and then used to fill borosilicate capillaries. Using a channel-cut Si(111) crystal monochromator the wavelength was set to be equal to 0.354496 \AA ; diffraction intensities were recorded by a bank of nine detectors, each preceded by a Si(111) crystal analyser.

Structure refinement. Structure refinements were performed using Rietveld methods through the GSAS package (Larson & von Dreele, 1994) with the EXPGUI interface (Toby, 2001). The structure reported by Hirano *et al.* (1992) was used as a starting model. The peak profile was fitted using the Thompson pseudo-Voigt function (Thompson *et al.*, 1987), while the background was refined using a Chebyshev polynomial function with 24 coefficients. Si—O distances were refined using 'soft constraints' [ok as edited?], gradually decreasing the weight of the constraint (up to 10 [unit?]) after the initial stages. Extra-framework species, cations and H_2O

Table 1

Chemical formulas of the whole sample set.

The error is calculated as $\text{error\%} = (\text{Al} - \text{K} - \text{NH}_4 - 3\text{Ce}) / (\text{K} + \text{NH}_4 + 3\text{Ce}) \times 100$ (Gottardi & Galli, 1985).

Name	Chemical analysis	Chemical formula	Error (%)
K-LTL	XRF, TGA	$\text{K}_{9.03}\text{Na}_{0.41}\text{Si}_{26.79}\text{Al}_{9.14}\text{O}_{72} \cdot 16.91 \text{H}_2\text{O}$	-3.2
Na-LTL	XRF, TGA	$\text{K}_{6.00}\text{Na}_{2.97}\text{Si}_{26.53}\text{Al}_{9.53}\text{O}_{72} \cdot 19.51 \text{H}_2\text{O}$	3.2
Na-LTL-80°C	XRF, LOI	$\text{K}_{6.00}\text{Na}_{2.93}\text{Si}_{26.75}\text{Al}_{9.30}\text{O}_{72} \cdot 19.60 \text{H}_2\text{O}$	4.3
NH ₄ -LTL	SEM-EDS, TGA, EA	$\text{K}_{2.25}(\text{NH}_4)_{6.86}\text{Si}_{26.91}\text{Al}_{9.08}\text{O}_{72} \cdot 17.07 \text{H}_2\text{O}$	-0.3
K-Ce-LTL	SEM-EDS, TGA	$\text{K}_{5.26}\text{Na}_{0.21}\text{Ce}_{1.16}\text{Si}_{26.63}\text{Al}_{9.50}\text{O}_{72} \cdot 20.26 \text{H}_2\text{O}$	6.1
Na-Ce-LTL	SEM-EDS, TGA	$\text{K}_{5.24}\text{Na}_{0.15}\text{Ce}_{1.26}\text{Si}_{26.55}\text{Al}_{9.55}\text{O}_{72} \cdot 20.53 \text{H}_2\text{O}$	4.2
NH ₄ -Ce-LTL	SEM-EDS, TGA, EA	$\text{K}_{1.82}(\text{NH}_4)_{3.92}\text{Ce}_{1.17}\text{Si}_{26.90}\text{Al}_{9.05}\text{O}_{72} \cdot 20.94 \text{H}_2\text{O}$	-2.2
NH ₄ -Ce-LTL-rev	SEM-EDS, TGA, EA	$\text{K}_{1.87}(\text{NH}_4)_{6.81}\text{Ce}_{0.09}\text{Si}_{27.07}\text{Al}_{8.90}\text{O}_{72} \cdot 17.26 \text{H}_2\text{O}$	-0.6

Table 2

Unit-cell parameters.

Sample	<i>a</i> (Å)	<i>c</i> (Å)	<i>V</i> (Å ³)
K-LTL	18.37294 (5)	7.52458 (3)	2199.74 (1)
Na-LTL	18.37075 (7)	7.52661 (4)	2199.80 (1)
NH ₄ -LTL	18.42200 (5)	7.54096 (3)	2216.31 (1)
K-Ce-LTL	18.34930 (5)	7.52420 (4)	2193.97 (1)
Na-Ce-LTL	18.34758 (5)	7.52461 (3)	2193.67 (1)
NH ₄ -Ce-LTL	18.38740 (5)	7.54285 (3)	2208.55 (1)

molecules were located in the zeolite **pores** by careful inspection of the Fourier difference map of the electronic density; the species were assigned considering the bond distances, the site-occupancy factors and the mutual exclusion rules **for distances that are too short [ok as edited?]**.

3. Results

3.1. Chemical characterization

Fig. 2 shows the TGA for all the exchanged samples and the obtained water content is reported in Table S4 in the supporting information.

The first peak of all the **DTG [please define]** curves, positioned below 300°C, represents the water loss, while peaks at higher temperatures, observed only for samples NH₄-LTL and NH₄-Ce-LTL, are related to the ammonium content. In particular, the peak near 650°C in the NH₄-LTL DTG (Fig. 2) curve could derive from the condensation of residual H⁺ ions.

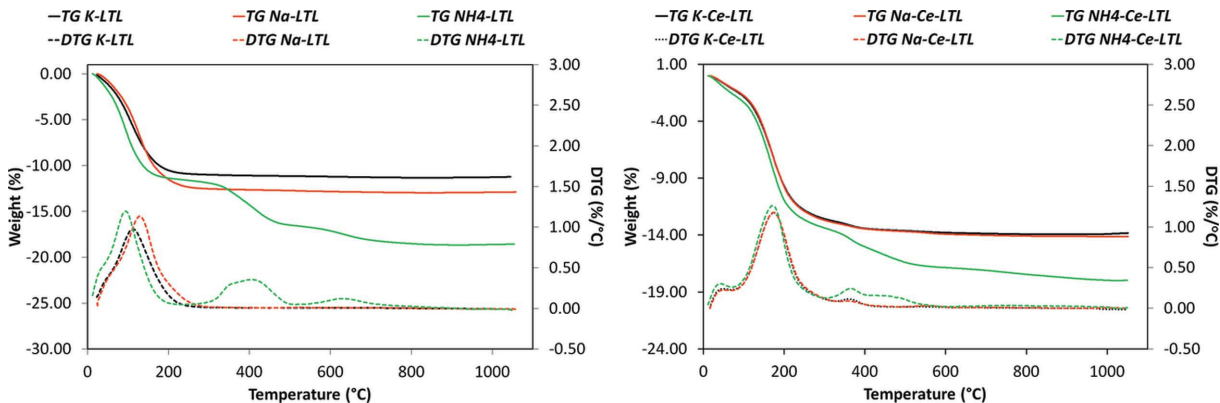


Figure 2

TGA (solid line) and DTG (dotted line) curves for: K-LTL, Na-LTL and NH₄-LTL samples in black, red and green, respectively (left panel), and K-Ce-LTL, Na-Ce-LTL and NH₄-Ce-LTL samples in black, red and green, respectively (right panel).

Table 1 reports the chemical formulas of the whole sample set, obtained considering: (i) the results obtained from XRF or SEM-EDS (Tables S1 and S2 in the supporting information); (ii) the NH₄ amount determined by elemental analysis (Table S3); (iii) the H₂O content (Table S4) determined by **TGA** or LOI analyses.

The chemical compositions reported in Table 1 give a clear idea about the exchange capacity of the samples involved in this study. From the comparison of the two Na-exchanged samples at different temperatures, it is possible to conclude that this variable is not critical in the improvement of the exchange effectiveness, as the two samples present the same final composition. For this reason, all the other experiments were performed at room temperature. Comparing Na-LTL and NH₄-LTL, we can deduce that the exchange is higher for NH₄ than for Na (2.25 and 6.00 potassium ions are not exchanged **from** the initial 9.03 in the two samples, respectively). Once the samples are exchanged with Ce³⁺ no clear affinity between Ce and one of the three cationic forms is observed. The three Ce³⁺-exchanged samples show, in fact, a similar amount of Ce (ranging from 1.16 to 1.26 atom **p.u.c. [please define]**), and also almost the same amount of H₂O molecules.

In order to recover Ce from zeolite **pores**, NH₄-Ce-LTL was further exchanged with a NH₄⁺ solution. The amount of Ce³⁺, obtained by EA, in the final NH₄-Ce-LTL-rev (0.09 p.u.c.) was compared with that of the NH₄-Ce-LTL (1.17 p.u.c.) proving the almost complete release of Ce and the restoration of the initial amount of ammonium as well as the H₂O molecules.

3.2. Structure analysis

Structure analysis was performed to determine the amount and position of the extra-framework species, in particular of Ce, in the zeolite **pores**, and to understand the guest–guest and host–guest interactions. Cell parameters are reported in Table 2; structural data, as well as refinement details and diffraction

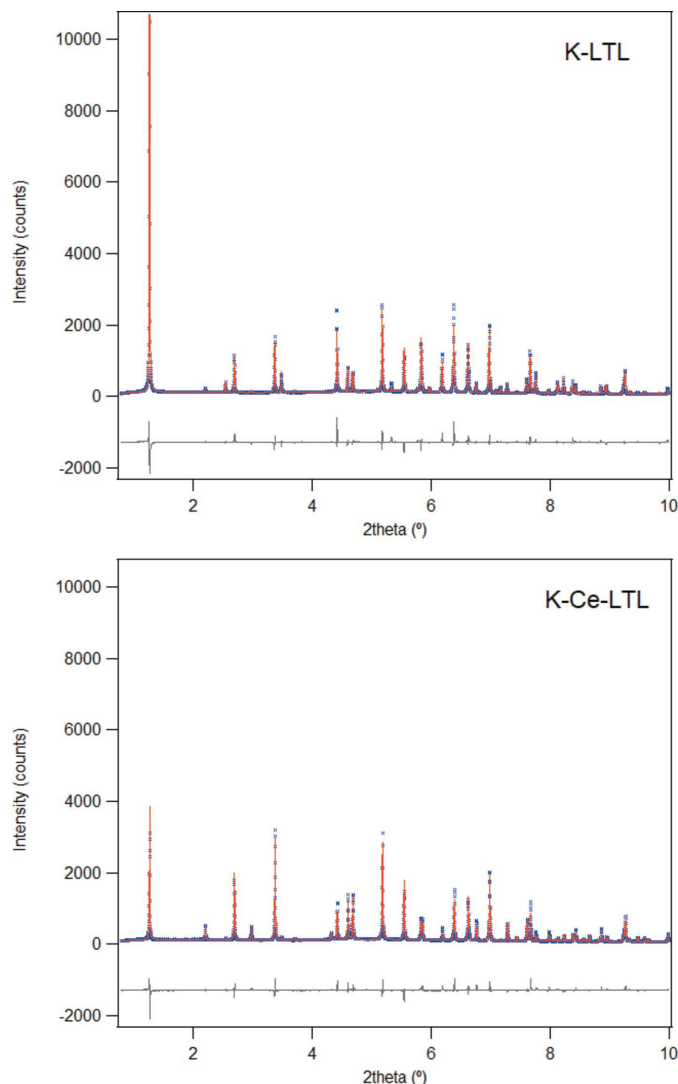


Figure 3
Zoomed-in view of observed (blue symbols) and calculated (red line) diffraction patterns and final difference curve (grey line) from Rietveld refinement of K-LTL and K-Ce-LTL.

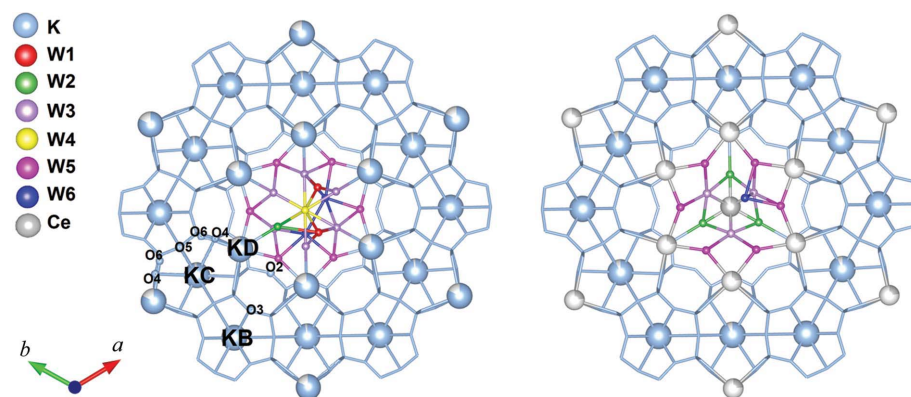


Figure 4
Structure of K-LTL (left panel) and K-Ce-LTL (right panel). Cations are drawn as incomplete spheres as a function of their fractional occupancies. For the H₂O molecules, only the positions actually occupied are shown, rather than all the partially occupied symmetrically equivalent positions.

patterns are reported in Tables S5–S17 and in Figs. S1–S6 in the supporting information. For selected samples (K-LTL and K-Ce-LTL), observed and calculated diffraction patterns obtained by Rietveld refinement are reported in Fig. 3.

3.2.1. Na⁺ and NH₄⁺ exchange. K-LTL and Na-LTL show very similar unit-cell parameters (Table 2), while we can observe slightly higher values for NH₄-LTL. Apart from this, the Ce-free cationic forms of zeolite L display similar structures (Tables S6–S11). No new extra-framework sites were located compared with those reported in the literature (see Section 2.1); all the cations are sited in the KB (at the centre of the cancrinite cage), KC (at the centre of the elliptical 8MR channel) and KD (close to the wall of the 12MR channel) sites [see the structure of K-LTL (Fig. 4, left panel)]. KB is bonded to the framework oxygen atoms O3 with six distances of about 2.9 Å and KC is placed at about 2.9 Å from four framework oxygen atoms O5 and at a larger distance from eight O4 atoms. Cations in KD, instead, display a solvation sphere constituted by W5 and W3 H₂O molecules and bonds with the framework oxygen atoms O4 and O6 (Fig. 4, left panel).

H₂O molecules are all placed in the main channel; they interact with each other, forming a cluster (Fig. 4, left panel). Two W4, at the centre of the 12MR channel, are at bonding distance and are also bonded to W1, W2, W3. Site W5, almost fully occupied in all samples, is located in the external part of the H₂O cluster at bonding distance with KD, W3 and W6. The only interaction between the framework oxygen atoms and H₂O molecules is observed for W2 with O1. In Table 3, the number of H₂O molecules in the six sites W1–W6 is reported for all the samples.

3.2.2. Ce³⁺ exchange. All the zeolites exchanged with Ce show a reduction of cell volume (due to the decrease of the *a* parameter) if compared with their Ce-free counterparts (Table 2). However, as already observed for the three Ce-free zeolites, NH₄-Ce-LTL shows a higher volume. When K, Na and NH₄ cations are exchanged with Ce, similar structural modifications occur in the three samples. All the patterns collected for Ce-exchanged samples show changes in the relative peak intensities compared with their Ce-free counterparts, especially in the low-angle region, clearly indicating different cation contents (see as an example NH₄-LTL and NH₄-Ce-LTL patterns in Fig. 5).

In the Ce-exchanged forms, in addition to KB, KC and KD cation sites, a new one appears in the middle of the 12MR channel (labelled Ce). In the Ce-exchanged samples the occupancy of KD and Ce sites was refined using the Ce scattering factor. The Ce site-occupancy factor ranges from 88 (K-Ce-LTL) to 97% (NH₄-Ce-LTL), indicating that this latter site is filled almost exclusively with Ce in all the exchanged zeolites (Fig. 4, right panel). This new site coordinates with W2 and W3. The

Table 3

H₂O p.u.c. in each W site for the whole sample set.

The low amount of H₂O found by XRPD in Ce-exchanged zeolites is explained in Section 4.

	K-LTL	Na-LTL	NH ₄ -LTL	K-Ce-LTL	Na-Ce-LTL	NH ₄ -Ce-LTL
W1	2.0	2.0	2.0			
W2	1.0	1.0	1.0	3.0	3.0	3.0
W3	6.0	6.0	6.0	6.0	6.0	6.0
W4	1.2	0.3	0.6			
W5	6.6	6.0	5.7	6.0	6.0	6.0
W6	1.8	2.5	1.6	1.0	1.0	1.0
Total	18.6	17.8	16.9	16	16	16

occupancy of site KD is about 20–22% for all the Ce-exchanged samples; thus it is impossible to exclude the presence of various cations in the same position. In the Ce-exchanged samples, H₂O molecules are positioned only in four sites W2, W3, W5 and W6 (Tables 3 and S12, S14, S16), creating a cluster that interacts slightly with the framework and bonding Ce site.

4. Discussion

4.1. Na⁺ and NH₄⁺ exchange

The K, Na and NH₄ zeolites show similar structures, but the occupancy factors of sites KB, KC and KD are different due to the different types and amount of exchanged extra-framework cations. Combining the information obtained by XRPD and chemical analysis (Table 4), we can assume the cation distribution in the three sites reported in Table 5. Since it is not possible to distinguish between different cations occupying the same site from the XRPD data, the comparison between XRPD and chemical data reported in Table 4 is only based on the number of electrons.

K-LTL presents a certain amount of Na (0.41 p.u.c.) which remains in part in all the exchanged samples, with the

exception of the NH₄-exchanged one (see Table 1) where NH₄ is able to remove all the Na. Since the KB site is always occupied by non-exchangeable K, these Na ions should be distributed in KC and KD sites. Na-LTL zeolite shows an exchange Na⁺ → K⁺ of about 27%, according to Sato *et al.* (1990), so we hypothesize a prevalent substitution of K ions in the main channel (KD), while the small amount of Na⁺ in KC is that already present in the pristine K-LTL. In sample NH₄-LTL, K⁺ ions are found mainly in the KB site and partially in KC, with an exchange NH₄⁺ → K⁺ of about 73%, in very good agreement with the results reported by Dyer *et al.* (1993). The higher value of this last exchange seems related to the ionic radii of the species involved (Dyer *et al.*, 1993). Indeed, NH₄⁺ and K⁺ show a more similar size when compared with the couple Na⁺–K⁺; thus NH₄⁺ can enter in site KD without affecting the framework stability. The presence of NH₄⁺ ions both in the 8MR and 12MR channels is also demonstrated by the broad peak (between 290 and 450°C) in DTG data related to the NH₄⁺ loss (Fig. 2). Indeed, the two sites occupied by this cation present different interactions with the framework and extra-framework species and hence **exhibit** different temperatures of release. In addition, in NH₄-LTL, we can notice an enlargement of the cell volume, and that site KD is positioned farther from the framework in comparison with the other samples (*i.e.* KD–O4 = 3.18 and 3.20 Å in K-LTL and Na-LTL, **respectively?**, and 3.25 in NH₄-LTL; KD–O6 = 2.98 and 2.99 Å in K-LTL and Na-LTL, **respectively?**, and 3.11 in NH₄-LTL). This can be a direct consequence of the slightly larger ionic radius of NH₄⁺ (1.40 Å) (Sidey, 2016) compared with K⁺ (1.37 Å) (Shannon, 1976) and Na⁺ (0.99 Å) (Shannon, 1976) and/or due to the hydrogen bonds occurring between the framework oxygen atoms and this cation.

Regarding H₂O molecules, in NH₄-LTL the shift towards lower temperature of the first peak of the DTG curve (Fig. 2), related to H₂O loss, can be caused by longer bonds between W2 and the framework [W2–O1 is 2.65 (6) Å in K-LTL, 2.61 (7) Å in Na-LTL and 2.81 (6) Å in NH₄-LTL]. In general, for all the samples, the total amount of cations and H₂O

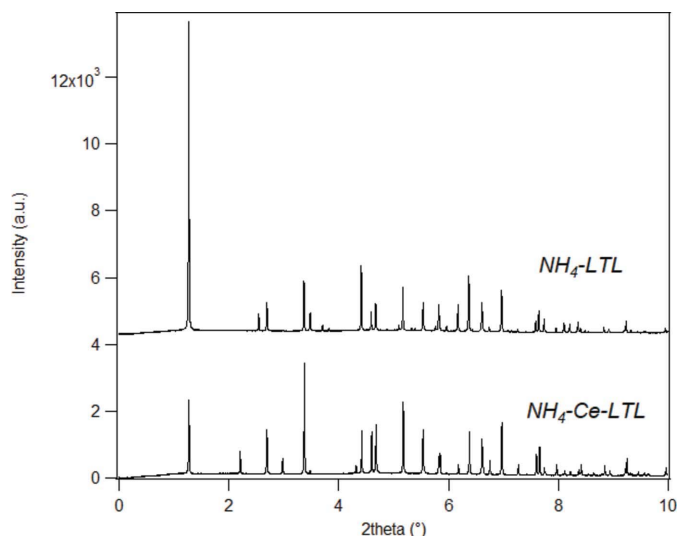


Figure 5
XRPD patterns of NH₄-LTL and NH₄-Ce-LTL.

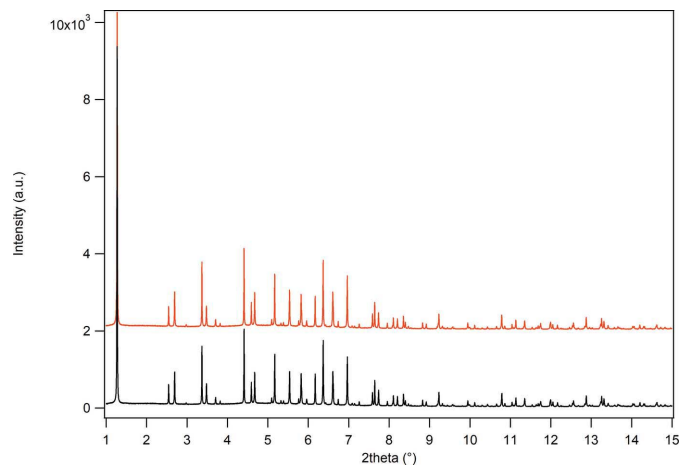


Figure 6
Comparison of XRPD patterns of NH₄-LTL (red line) and NH₄-Ce-LTL-rev, after Ce recovery (black line) samples.

Table 4

Number of electrons (e) for cations (cat.) and H₂O molecules derived from structural (XRPD) (number of atoms × Z depending on the scattering factor used for the occupancy factor refinement of each cation site) and chemical analyses (number of atoms from the chemical formula × Z). The differences between the total number of electrons for cations and H₂O molecules obtained by the two techniques are also reported (e cat. XRPD – e cat. chemical analysis; e H₂O XRPD – e H₂O chemical analysis).

	XRPD						Chemical analysis						e Dif. cat.	e Dif. H ₂ O
	e KB	e KC	e KD	e Ce	e cat.	e H ₂ O	e K	e Na	e NH ₄	e Ce	e cat.	e H ₂ O		
K-LTL	36.00	51.30	89.64		176.94	148.43	162.54	4.10			166.64	135.28	10.30	13.14
Na-LTL	36.00	50.76	69.12		155.88	142.88	108.00	29.70			137.70	156.00	18.18	−13.12
NH ₄ -LTL	36.00	28.08	57.24		121.32	135.02	40.50		68.60		109.10	136.56	12.22	−1.53
K-Ce-LTL	36.00	50.22	75.90	48.51	210.63	127.99	94.68	2.10		63.80	160.58	162.08	50.05	−34.08
Na-Ce-LTL	36.00	50.76	75.90	53.90	216.56	128.00	94.32	1.50		69.30	165.12	164.24	51.44	−36.24
NH ₄ -Ce-LTL	34.92	28.62	66.00	52.80	182.34	127.97	32.76		39.20	64.35	136.31	167.52	46.03	−39.55

Table 5

Cation distribution over the extra-framework sites deduced from structural and chemical results.

		K		Na		NH ₄		Ce	
		e	Atom	e	Atom	e	Atom	e	Atom
K-LTL	KB	36.00	2.00						
	KC	51.90	2.88	2.10	0.21				
	KD	74.64	4.15	2.00	0.20				
Na-LTL	KB	36.00	2.00						
	KC	52.50	2.92	1.50	0.15				
	KD	19.50	1.08	28.2	2.82				
NH ₄ -LTL	KB	36.00	2.00						
	KC	4.50	0.25			27.50	2.75		
	KD					41.10	4.11		
K-Ce-LTL	KB	36.00	2.00						
	KC	48.12	2.67	2.10	0.21			15.29	0.28
	KD	10.56	0.59					48.51	0.88
Na-Ce-LTL	Ce								
	KB	36.00	2.00						
	KC	49.26	2.74	1.50	0.15				
NH ₄ -Ce-LTL	KD	9.06	0.50					15.40	0.28
	Ce							53.90	0.98
	KB	32.76	1.82						
NH ₄ -Ce-LTL	KC					28.62	2.86		
	KD					10.58	1.06	11.55	0.21
	Ce							52.80	0.96

molecules obtained by structural refinement is in good agreement with those values resulting from chemical analysis (Table 4). In sample Na-LTL, the number of cations from structure refinement is slightly overestimated, but this could be due to the simultaneous presence of cations and H₂O molecules on the KD site. This is consistent with the finding that the number of H₂O molecules obtained is underestimated with respect to the TGA data. The fact that KD can be shared by the different species (also **the case** in the other samples) is also suggested by the high value of its thermal parameter.

4.2. Ce³⁺ exchange and recovery

All Ce-exchanged zeolites show a similar amount of Ce p.u.c. (1.1–1.2 atoms p.u.c.) (Table 1) (exchange degree from 38% to 42%) and similar cation distribution. On the basis of the cation distribution reported in Table 5, Ce mainly occupies the site Ce and, to a lesser extent, site KD. From Table 4, structural analysis always shows an overestimation of the cations, accompanied by an underestimation of the number of H₂O molecules. Thus, we can assume that the cation over-

estimation is due to the co-presence of H₂O molecules in sites Ce and KD; **these H₂O molecules [ok as edited?]** have migrated from the original sites W1 and W4, which are empty in these samples. This hypothesis is confirmed by the high thermal parameters of these two sites, indicating a high degree of structural disorder. In comparison with the pristine materials, Ce-exchanged zeolites show a higher amount of H₂O (Table 1), according to: (i) the bigger solvation sphere of this cation [solvation spheres: Ce³⁺ = 9.1 (Lutz *et al.*, 2012), K⁺ = 7.5 (Duignan *et al.*, 2020), NH₄⁺ = 5.8 (Chang & Dang, 2003), Na⁺ = 5.6 H₂O molecules (Duignan *et al.*, 2020)]; (ii) the larger space available due to the lower amount of trivalent cations present in the main channel. The H₂O content is similar for the three samples, due to the same amount of Ce incorporated, as well as the temperature of its release (see the first two peaks of the

DTG, Fig. 2). It is interesting to observe that these temperatures appear higher than in pristine materials, due to the strong and short bonds occurring between the Ce site and W2 and W3 (respectively, about 2.3 and 2.6 Å). Ce penetration, indeed, leads to a reorganization of the position of the H₂O molecules and their bonds with this element have a different coordination sphere with respect to the original K⁺, Na⁺ and NH₄⁺ cations. This, beyond the intrinsic properties of zeolite L, can play an important role in the exchange capacity.

The complete recovery of cerium from the NH₄-Ce-LTL was achieved through a further exchange with a NH₄ solution. Chemical results demonstrated complete recovery of the initial amount of ammonium and water molecule in the zeolite with an almost complete release of cerium. As further demonstration, the two XRPD patterns, reported in Fig. 6, of the initial NH₄-LTL and the NH₄-Ce-LTL-rev after cerium recovery show the same features, suggesting the same structure and the same type and number of cations.

5. Conclusions

The aim of this work was the evaluation of the Ce-exchange capacity of three cationic forms of LTL zeolites (the as-synthesized K form and Na- and NH_4 -exchanged ones) using a highly concentrated solution of Ce. The effect of the Ce exchange in the different cationic forms was evaluated through chemical analyses and XRPD structural investigations. Indeed, structural studies can give new insight into the sites involved in the exchange, and this is fundamental for the choice of a powerful protocol of exchange for future application such as Ce recovery from diluted solution. The results reported here also have important implications for catalytic applications, since many zeolite catalysts are prepared through Ce exchange.

The obtained results show a $\text{Na}^+ \rightarrow \text{K}^+$ substitution of about 27%, while $\text{NH}_4^+ \rightarrow \text{K}^+$ reached 73%, because the cations in the extra-framework site KC – in the 8MR channel – are exchanged only if K^+ is replaced by NH_4^+ ions due to their similar ionic size. The cation-exchange degree for Ce ranges from 38 to 42% and the LTL cation-exchange capacity for Ce is not influenced by the nature of the cations in the pristine sample. In contrast to what was observed for Na and NH_4 exchange, in which the cations occupy the pre-existing potassium positions, the Ce cations occupy a new site in the 12MR site and induce a reorganization of the H_2O molecules. This may be due to the higher ionic potential of Ce atoms, which tend to form a stronger solvation sphere that hinders cation mobility. The Ce-exchange capacity of zeolite L and its affinity with this element can thus be driven not only by the intrinsic property of the LTL framework, but also by the coordination sphere of Ce compared with the original K^+ , Na^+ and NH_4^+ cations. With the aim of possible REE recovery from zeolite **pores**, the Ce-exchanged NH_4 -LTL was tested through exchange with a NH_4^+ solution, leading to the 100% recovery of this element. The results presented here are promising for future Ce-recovery experiments from very diluted solutions.

Acknowledgements

The authors thank Massimo Tonelli, Michelangelo Polisi and Simona Bigi for their technical support, and Gianluca Malavasi for the laboratory equipment.

References

- Arletti, R., Fois, E., Gigli, L., Vezzalini, G., Quartieri, S. & Tabacchi, G. (2017). *Angew. Chem. Int. Ed.* **56**, 2105–2109.
- Arletti, R., Giacobbe, C., Quartieri, S. & Vezzalini, G. (2017). *Minerals*, **7**, 18.
- Baerlocher, C., McCusker, L. B. & Olson, D. H. (2007). *Atlas of Zeolite Framework Types*, 6th ed. Amsterdam, The Netherlands: Elsevier.
- Balaram, V. (2019). *Geosci. Front.* **10**, 1285–1303.
- Barrer, R. M. & Meier, W. M. (1958). *J. Chem. Soc.* p. 299.
- Barros, O., Costa, L., Costa, F., Lago, A., Rocha, V., Vipotnik, Z., Silva, B. & Tavares, T. (2019). *Molecules*, **24**, 1005.
- Bennett, J. M. & Smith, J. V. (1968). *Mater. Res. Bull.* **3**, 633–642.

- Binnemans, K., Jones, P. T., Müller, T. & Yurramendi, L. (2018). *J. Sustain. Met.* **4**, 126–146.
- Boekfa, B., Pantu, P. & Limtrakul, J. (2008). *J. Mol. Struct.* **889**, 81–88.
- Boer, M. A. de & Lammertsma, K. (2013). *ChemSuschem*, **6**, 2045–2055.
- Bryukhanov, I. A., Rybakov, A. A., Larin, A. V., Trubnikov, D. N. & Vercauteren, D. P. (2017). *J. Mol. Model.* **23**, 68.
- Chakhmouradian, A. R. & Wall, F. (2012). *Elements*, **8**, 333–340.
- Chang, T. M. & Dang, L. X. (2003). *J. Chem. Phys.* **118**, 8813–8820.
- Charalampides, G., Vatalis, K., Karayannis, V. & Baklavaridis, A. (2016). *IOP Conf. Ser.: Mater. Sci. Eng.* **161**, 012069.
- Charalampides, G., Vatalis, K. I., Apostoplos, B. & Ploutarch-Nikolas, B. (2015). *Procedia Econ. Financ.* **24**, 126–135.
- Confalonieri, G., Fabbiani, M., Arletti, R., Quartieri, S., Di Renzo, F., Haines, J., Tabacchi, G., Fois, E., Vezzalini, G., Martra, G. & Santoro, M. (2020). *Microporous Mesoporous Mater.* **300**, 110163.
- Confalonieri, G., Grand, J., Arletti, R., Barrier, N. & Mintova, S. (2020). *Microporous Mesoporous Mater.* **306**, 110394.
- Confalonieri, G., Quartieri, S., Vezzalini, G., Tabacchi, G., Fois, E., Daou, T. J. & Arletti, R. (2019). *Microporous Mesoporous Mater.* **284**, 161–169.
- Confalonieri, G., Ryzhikov, A., Arletti, R., Nouali, H., Quartieri, S., Daou, T. J. & Patarin, J. (2018). *J. Phys. Chem. C*, **122**, 28001–28012.
- Confalonieri, G., Ryzhikov, A., Arletti, R., Quartieri, S., Vezzalini, G., Isaac, C., Paillaud, J. L., Nouali, H. & Daou, T. J. (2020). *Phys. Chem. Chem. Phys.* **22**, 5178–5187.
- Coudert, F. X., Cailliez, F., Vuilleumier, R., Fuchs, A. H. & Boutin, A. (2009). *Faraday Discuss.* **141**, 377–398.
- Dejoie, C., Martinetto, P., Tamura, N., Kunz, M., Porcher, F., Bordat, P., Brown, R., Dooryhée, E., Anne, M. & McCusker, L. B. (2014). *J. Phys. Chem. C*, **118**, 28032–28042.
- Deshmane, V. G., Islam, S. Z. & Bhawe, R. R. (2020). *Environ. Sci. Technol.* **54**, 550–558.
- Diaz, L. A., Lister, T. E., Parkman, J. A. & Clark, G. G. (2016). *J. Clean. Prod.* **125**, 236–244.
- Duignan, T. T., Schenter, G. K., Fulton, J. L., Huthwelker, T., Balasubramanian, M., Galib, M., Baer, M. D., Wilhelm, J., Hutter, J., Del Ben, M., Zhao, X. S. & Mundy, C. J. (2020). *Phys. Chem. Chem. Phys.* **22**, 10641–10652.
- Duploux, L. (2016). PhD thesis, University of Helsinki, Université de Lille.
- Dyer, A. (2007). *Studies in Surface Science and Catalysis*, Vol. 168, edited by J. Čejka, H. van Bekkum, A. Corma & F. Schüth, pp. 525–553. **City of publication?**: Elsevier.
- Dyer, A., Amini, S., Enamy, H., El-Naggar, H. A. & Anderson, M. W. (1993). *Zeolites*, **13**, 281–290.
- Fabbiani, M., Confalonieri, G., Morandi, S., Arletti, R., Quartieri, S., Santoro, M., Di Renzo, F., Haines, J., Fantini, R., Tabacchi, G., Fois, E., Vezzalini, G., Ricchiardi, G. & Martra, G. (2021). *Microporous Mesoporous Mater.* **311**, 110728.
- Faghihian, H., Amini, M. K. & Nezamzadeh, A. R. (2005). *J. Radioanal. Nucl. Chem.* **264**, 577–582.
- Franzini, M., Leoni, L. & Saitta, M. (1975). *Rendiconti Società Italiana di Mineralogia e Petrologia*, **XXXI**, 365–378.
- Frising, T. & Leflaive, P. (2008). *Microporous Mesoporous Mater.* **114**, 27–63.
- Gad, H. M. H. & Awwad, N. S. (2007). *Sep. Sci. Technol.* **42**, 3657–3680.
- Gautam, P., Barman, S. & Ali, A. (2020). *Int. J. Chem. React. Eng.* **18**, 20200081.
- Gigli, L., Arletti, R., Quartieri, S., Di Renzo, F. & Vezzalini, G. (2013). *Microporous Mesoporous Mater.* **177**, 8–16.
- Gottardi, G. & Galli, E. (1985). *Natural Zeolites*. Berlin, Heidelberg: Springer-Verlag.
- Haque, N., Hughes, A., Lim, S. & Vernon, C. (2014). *Resources*, **3**, 614–635.
- Hirano, M., Kato, M., Asada, E., Tsutsumi, K. & Shiraishi, A. (1992). *Adv. X-ray Chem. Anal. Jpn.* **23**, 101–110.

- Hong, S. H., Jang, M. S., Cho, S. J. & Ahn, W. S. (2014). *Chem. Commun.* **50**, 4927–4930.
- Hudson, M. R., Queen, W. L., Mason, J. A., Fickel, D. W., Lobo, R. F. & Brown, C. M. (2012). *J. Am. Chem. Soc.* **134**, 1970–1973.
- Isaac, C., Confalonieri, G., Nouali, H., Paillaud, J. L., Arletti, R., Daou, T. J. & Ryzhikov, A. (2020). *Microporous Mesoporous Mater.* **298**, 110047.
- Jowitt, S. M., Werner, T. T., Weng, Z. H. & Mudd, G. M. (2018). *Curr. Opin. Green Sustain. Chem.* **13**, 1–7.
- Kavun, V., van der Veen, M. A. & Repo, E. (2021). *Microporous Mesoporous Mater.* **312**, 110747.
- Kooten, W. E. J. van, Calis, H. P. A. & van den Bleek, C. M. (1998). *Catal. Automot. Pollut. Contr. IV*, **116**, 357–366.
- Krohn, J. E. & Tsapatsis, M. (2005). *Langmuir*, **21**, 8743–8750.
- Larson, A. C. & Von Dreele, R. B. (1994). **Reference details?**
- Leoni, L. & Saitta, M. (1976). *Rendiconti Societa' Italiana di Mineralogia e Petrologia*, **32**, 497–510.
- Lu, C. Y., Bai, H. L., Wu, B. L., Su, F. S. & Hwang, J. F. (2008). *Energy Fuels*, **22**, 3050–3056.
- Lutz, O. M. D., Hofer, T. S., Randolph, B. R. & Rode, B. M. (2012). *Chem. Phys. Lett.* **539–540**, 50–53.
- Manos, M. J. & Kanatzidis, M. G. (2016). *Chem. Sci.* **7**, 4804–4824.
- Massari, S. & Ruberti, M. (2013). *Resour. Policy*, **38**, 36–43.
- Meshram, P. & Abhilash (2020). *Miner. Process. Extr. Metall. Rev.* **41**, 279–310.
- Mosai, A. K., Chimuka, L., Cukrowska, E. M., Kotzé, I. A. & Tutu, H. (2019). *Water Air Soil Pollut.* **230**, 188.
- Ni'Am, A. C., Wang, Y. F., Chen, S. W., Chang, G. M. & You, S. J. (2020). *Chem. Eng. Process.* **148**, 107831.
- Pabalan, R. T. & Bertetti, F. P. (2001). *Rev. Mineral. Geochem.* **45**, 453–518.
- Porvali, A., Wilson, B. P. & Lundström, M. (2018). *Waste Manage. (Oxford)*, **71**, 381–389.
- Rademaker, J. H., Kleijn, R. & Yang, Y. X. (2013). *Environ. Sci. Technol.* **47**, 10129–10136.
- Royen, H. & Fortkamp, U. (2016). *Report of IVL Swedish Environmental Research Institute 2016*.
- Saada, M. A., Soulard, M., Marler, B., Gies, H. & Patarin, J. (2011). *J. Phys. Chem. C*, **115**, 425–430.
- Santoro, M., Ciabini, L., Bini, R. & Schettino, V. (2003). *J. Raman Spectrosc.* **34**, 557–566.
- Santoro, M., Scelta, D., Dziubek, K., Ceppatelli, M., Gorelli, F. A., Bini, R., Garbarino, G., Thibaud, J. M., Di Renzo, F., Cambon, O., Hermet, P., Rouquette, J., van der Lee, A. & Haines, J. (2016). *Chem. Mater.* **28**, 4065–4071.
- Sato, M., Morikawa, K. & Kurosawa, S. (1990). *Eur. J. Mineral.* **2**, 851–860.
- Scelta, D., Ceppatelli, M., Santoro, M., Bini, R., Gorelli, F. A., Perucchi, A., Mezouar, M., van der Lee, A. & Haines, J. (2014). *Chem. Mater.* **26**, 2249–2255.
- Shannon, R. D. (1976). *Acta Cryst.* **A32**, 751–767.
- Sidey, V. (2016). *Acta Cryst.* **B72**, 626–633.
- Simoncic, P. & Armbruster, T. (2004). *Am. Mineral.* **89**, 421–431.
- Stückenschneider, K., Merz, J., Hanke, F., Rozyczko, P., Milman, V. & Schembecker, G. (2013). *J. Phys. Chem. C*, **117**, 18927–18935.
- Thompson, P., Cox, D. E. & Hastings, J. B. (1987). *J. Appl. Cryst.* **20**, 79–83.
- Toby, B. H. (2001). *J. Appl. Cryst.* **34**, 210–213.
- Zhang, K., Lively, R. P., Noel, J. D., Dose, M. E., McCool, B. A., Chance, R. R. & Koros, W. J. (2012). *Langmuir*, **28**, 8664–8673.
- Zhou, H. Y., Wang, Y. L., Guo, X. G., Dong, Y. M., Su, X. & Sun, X. Q. (2018). *J. Mol. Liq.* **254**, 414–420.



ISSN: 1600-5767

YOU WILL AUTOMATICALLY BE SENT DETAILS OF HOW TO DOWNLOAD
AN ELECTRONIC REPRINT OF YOUR PAPER, FREE OF CHARGE.
PRINTED REPRINTS MAY BE PURCHASED USING THIS FORM.

Please scan your order and send to ls@iucr.org

INTERNATIONAL UNION OF CRYSTALLOGRAPHY

5 Abbey Square
Chester CH1 2HU, England.

VAT No. GB 161 9034 76

Article No.: J211082-VB5024

Title of article Ce-exchange capacity of zeolite L in different cationic forms: a structural investigation

Name Giorgia Confalonieri

Address ID22 Beamline, European Synchrotron Radiation Facility (ESRF), 71 Av. des Martyrs, Grenoble, 38000, France

E-mail address (for electronic reprints) giorgia.confalonieri@esrf.fr

OPEN ACCESS

IUCr journals offer authors the chance to make their articles open access on **Crystallography Journals Online**. If you wish to make your article open access please go to <https://scripts.iucr.org/openaccess/?code=VB5024>

The charge for making an article open access is from **1600 United States dollars** (for full details see <https://journals.iucr.org/j/services/openaccess.html>). For authors in European Union countries, VAT will be added to the open-access charge.

DIGITAL PRINTED REPRINTS

I wish to order paid reprints

These reprints will be sent to the address given above. If the above address or e-mail address is not correct, please indicate an alternative:

PAYMENT (REPRINTS ONLY)

Charge for reprints USD

☐ An official purchase order made out to **INTERNATIONAL UNION OF CRYSTALLOGRAPHY** ☐ is enclosed ☐ will follow

Purchase order No.

☐ Please invoice me

☐ I wish to pay by credit card

EU authors only: VAT No:

Date

Signature

OPEN ACCESS

The charge for making an article open access is from **1600 United States dollars** (for full details see <https://journals.iucr.org/j/services/openaccess.html>). For authors in European Union countries, VAT will be added to the open-access charge.

DIGITAL PRINTED REPRINTS

An electronic reprint is supplied free of charge.

Printed reprints without limit of number may be purchased at the prices given in the table below. The requirements of all joint authors, if any, and of their laboratories should be included in a single order, specifically ordered on the form overleaf. All orders for reprints must be submitted promptly.

Prices for reprints are given below in **United States dollars** and include postage.

Number of reprints required	Size of paper (in printed pages)				
	1–2	3–4	5–8	9–16	Additional 8's
50	184	268	372	560	246
100	278	402	556	842	370
150	368	534	740	1122	490
200	456	664	920	1400	610
Additional 50's	86	128	178	276	116

PAYMENT AND ORDERING

Official purchase orders should be made out to **INTERNATIONAL UNION OF CRYSTALLOGRAPHY**.

Orders should be returned by email to ls@iucr.org

ENQUIRIES

Enquiries concerning reprints should be sent to support@iucr.org.